Properties of C−C Bonds in *n*-Alkanes: Relevance to Cracking Mechanisms

Ken C. Hunter and Allan L. L. East*

Department of Chemistry and Biochemistry, University of Regina, Regina, Saskatchewan S4S 0A2, Canada

Received: July 26, 2001; In Final Form: October 11, 2001

The slight variations among the proton affinities and bond strengths of the C−C bonds in straight-chain *n*-alkanes have been determined to 1 kcal mol^{-1} accuracy for the first time, using computational quantum chemistry. Four computational methods (B3LYP, MP2, CCSD(T), and G2) were used to study *n*-alkanes (up to $C_{20}H_{42}$ with B3LYP), including computations on the related alkyl radicals, carbenium ions, and carbonium ions. The proton affinities of the C−C bonds vary from 142 to over 166 kcal mol^{-1}, are highest for the center C−C bond, and decrease monotonically toward the end bonds. Bond strength, unlike proton affinity, is very constant (88 kcal mol^{-1}), except for the α and β bonds (89 and 87 kcal mol^{-1}, respectively). For thermal cracking, the results suggest that the most favored initiation step is the breaking of the β bond of the alkane to create an ethyl radical. For Bronsted-acid-catalyzed cracking of straight-chain paraffins, if the initiation mechanism is via carbonium ions, then the results indicate that the central C−C bonds of *n*-alkanes will be most attractive to the Bronsted proton. However, for direct protolysis (Bronsted-mediated fission) of an *n*-alkane via a carbonium intermediate, the net exothermicities do not strongly discern among the C−C bonds. Trends in molecular geometry and infrared spectra features are also presented, and a signature IR band is predicted for carbonium ions that should aid in their identification.

Introduction

Petroleum refining and modification has featured strong research activity throughout the 20th century. Two significant driving forces for current research are the search for economical ways to tap the difficult sources of petroleum, such as tar sands, and the efforts to provide more environmentally friendly ways of performing the refining. One example of current research is the plethora of experiments that specifically test new catalysts for cracking of alkanes (paraffins, the largest component of petroleum) into smaller, more useful fragments. While current industrial processes use zeolites as their catalysts of choice, research is ongoing with other possibilities, including newer zeolites, other molecular sieves, and ionic liquids.

Many of the steps in the chemical mechanisms for alkane cracking are understood in a general sense, but some of the details are still unknown. For instance, in both thermal cracking and acid-catalyzed cracking, a monomolecular β-scission rule is well-known and generally accounts for most of the C−C-bond cracking.[1,2] In thermal cracking the β-scission occurs with alkyl radicals, while in acid-catalyzed cracking it occurs with alkyl cations (carbenium ions):
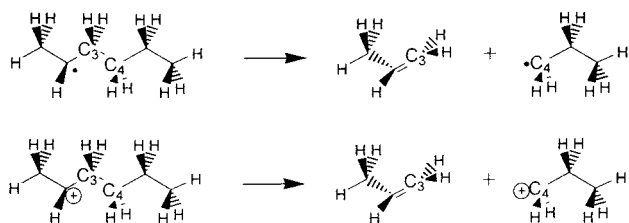
However, other aspects of the overall mechanisms that are still under debate include the initiation steps that create the alkyl radicals or carbenium ions and possible alternative steps for C−C-bond fission that might be simultaneously occurring.

Initiation Steps. In the case of thermal cracking of alkanes, the initiation step seems fairly well understood to be C−C bond fission to form two radicals, with the preferred C−C ruptures occurring between the most highly substituted carbons. However, we found a calculation of relative C−C-bond initiation rates for the pyrolysis of *n*-hexane,[3] based on heats of formation and other assumptions, which curiously suggested that not all C−C bonds between secondary carbons are equally probable to undergo the initiation step. In particular, dissociation to C_2H_5 and C_4H_9 radicals was derived to occur 10 times faster than dissociation to two C_3H_7 radicals. We are unaware of any theoretical explanation for why this should be so.

In the case of acid-catalyzed cracking of alkanes, the initiation steps have been the sources of a great deal of discussion for many years. Four possible activation mechanisms for the generation of the active carbenium ions have been discussed. The *abstraction initiation* idea features a Lewis-acid catalyst stripping a hydride (H$^-$) from an alkane to create a carbenium ion.[4,5] The *redox initiation* idea features an oxidizing catalyst stripping an electron from an alkane, with the alkane radical cation further decomposing to create a carbenium ion.[6,7] The *alkene initiation* idea features the protonation by the catalyst of trace amounts of alkene in the feed, creating carbenium ions.[5,8] The *carbonium initiation* idea features the protonation by the catalyst of alkanes themselves, forming unstable carbonium entities which dissociate to form carbenium ions.[9,10] The formed carbenium ion may or may not be covalently bonded to another species (e.g. a zeolite surface); for sake of generality we will ignore this complication here.

The carbonium mechanism, in particular, is seeing increased research interest, with new experiments[11−17] but particularly with computational chemistry methods.[17−35] Carbonium ions, or protonated alkanes, were first detected in mass spectrometry

Properties of C−C Bonds in *n*-Alkanes

J. Phys. Chem. A, Vol. 106, No. 7, 2002 **1347**

experiments[36] and have been spectroscopically detected only in the gas phase. They are highly reactive ions that are difficult to study experimentally due to their short chemical lifetime, and theoretical chemistry has therefore become the most valuable tool for their investigation. Computational studies of these gas-phase ions have demonstrated stable minima featuring 3-center−2-electron bonds. Two of the three general isomers of $C_2H_7^+$ ion have been detected in the gas phase.[37] Proponium and butonium ions have been recently studied computationally by Mota and co-workers,[22,38,39] demonstrating multiple possible geometries for protonation, as well as providing useful energetics. Calculations on larger carbonium ions have been limited in accuracy and/or scope.[18,20,29,40−43] Several computational studies have investigated the catalytic carbonium initiation mechanism directly, by attempting to model actual catalytic events involving carbonium ion formation,[17,19,21,24−28,30−34] and although these models all suffer from incomplete treatment of long-range effects,[34] they have resulted in one intriguing suggestion−that carbonium ions in condensed phases are not intermediates but transition states.[35] Three of the outstanding questions regarding the carbonium initiation mechanism are the following: why does the proton attack some alkanes but not others, where on an alkane does the catalytic proton attack, and how exactly do these carbonium ions produce carbenium ions?

Alternative Steps for C−C-Bond Fission. Under certain conditions for acid-catalyzed cracking, several experiments have shown strong evidence[13,15,44,45] that C−C-bond cracking can directly occur via carbonium ions (protonated alkanes):
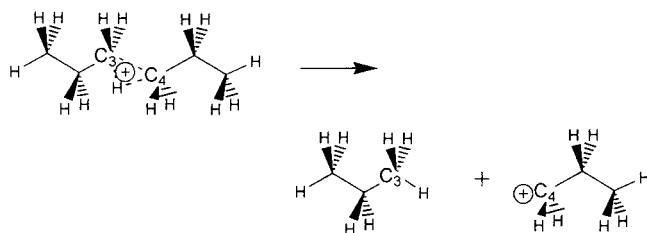
Gas-phase calculations have demonstrated that σ_{C-C}-bond protonation dramatically weakens the C−C bond strength (from approximately 88 to 8 kcal mol^{-1} for secondary carbons; vide supra). However, this carbonium decomposition route is in competition with the alternate route of σ_{C-H} protonation followed by loss of H_2, and these rapid steps are difficult to detect experimentally. For better evidence of this alternative C−C bond fission hypothesis, predicted product distributions for σ_{C-C} protonation might be of use, and this would require more data and work from computational quantum chemists.

The mechanistic questions mentioned above are all fundamentally linked to the molecular properties of the alkanes themselves. This paper is intended to foster this link. This theoretical (computational) study addresses the properties of the C−C bonds of a class of alkanes (*n*-alkanes) and connects them to the discussions of the postulated initiation steps of petroleum modification. Although *n*-alkanes may seem at first rather mundane, our examination of them appears to be the first serious attempt at detecting differences among their C−C bonds. We examined two processes. The first, relevant to thermal cracking, was C−C dissociation to form primary radicals. The second, relevant to Bronsted-acid-catalyzed cracking, was C−C protonation to form carbonium ions and ensuing dissociation to form carbenium ions. As far as we are aware, this study is the first to look at the trends in C−C bond properties with position on the alkane chain, and with length of chain.

Theoretical Methods

All calculations were performed with the software suite Gaussian 98.[46] Molecular geometries (opt = tight) and harmonic frequencies were computed using analytic 1st and 2nd derivative formulas as is routine with Gaussian 98, and zero-point vibrational energies (ZPVE) and thermal energy corrections were computed using the rigid-rotor/harmonic oscillator approximations, unscaled harmonic frequencies (except for the G2 method; see below), and standard statistical thermodynamic formulas.[47] Open-shell species were calculated with the unrestricted (UHF) orbital formalism throughout.

Four levels of electronic structure theory were employed. The first, B3LYP, is a semiempirical density functional theory (DFT) model parametrized by Becke[48] in which the exchange functional is a linear combination of the Hartree−Fock exchange with two functionals more traditional to DFT, and the correlation functional is that of Lee, Yang, and Parr.[49] The B3LYP calculations employed the 6-31G(d,p) basis set[46] and were applied for molecules having up to 20 carbons. We note that the use of the default numerical grid for the DFT integrals led to bad numerical noise in the vibrational frequency calculations for the long alkanes and, hence, the "ultrafine" grid of Gaussian 98 was used in all B3LYP calculations.

The second level of theory, MP2, is second-order Møller−Plesset perturbation theory, an ab initio method.[50] The MP2 calculations also used the 6-31G(d,p) basis set and were applied for molecules having up to 10 carbons. The vibrational frequency noise was quite acceptable, since all integrals were analytic. The frozen-core approximation was employed.

The third level of theory, called G2 or Gaussian2, is a high-accuracy method which takes a large-basis-set MP2 result and computes several energy corrections for electron correlation, plus a zero-point energy correction and a semiempirical correction based on the number of odd electrons.[51] The geometry is optimized using MP2, and the vibrational frequencies are scaled from Hartree−Fock-calculated values. The G2 method was employed for molecules having up to 6 carbons.

The fourth level of theory, CCSD(T), is coupled-cluster theory with single, double, and approximate triple excitations and is a high-accuracy ab initio method.[52−54] The CCSD(T) calculations used the cc-pVTZ basis set[55] and the frozen-core approximation and were applied to molecules having up to 6 carbons. The reported CCSD(T) energies were computed at MP2/6-31G(d,p) geometries and used ZPVE and thermal corrections from the B3LYP calculations.

Calculations were performed for alkanes, primary alkyl radicals, carbonium ions, and "primary" carbenium ions. Only the all-trans forms of the molecules and ions were examined, so that the C_nH_{2n+2} alkanes had either D_{2h} (*n* even) or C_{2v} (*n* odd) symmetry. The primary radicals had C_s symmetry, despite our occasional need to begin the optimizations in C_1 symmetry for convergence reasons. For the carbonium ions ($C_nH_{2n+3}^+$), protonation of the C−C bonds was done from a direction perpendicular to the plane of the carbon atoms. This resulted in C_{2h} symmetry for protonation of the central C−C bond in D_{2h} alkanes and C_1 symmetry for protonation of off-center C−C bonds.

For the carbenium ions ($C_nH_{2n+1}^+$), which under most laboratory conditions normally rearrange to form secondary or branched isomers, we were able to find a systematic set of local minima that *most closely represent* the hypothetical "primary carbenium ions" which would first result from dissociation of an all-trans *n*-carbonium ion. This optimized structure was labeled a "protonated alkylcyclopropane" by Sieber, Schleyer,
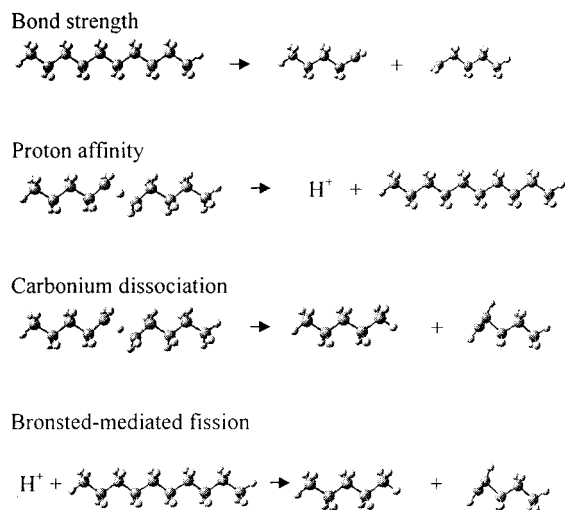
Bond strength

Proton affinity

Carbonium dissociation

Bronsted-mediated fission

Figure 1. Exemplary structures of molecules and reactions encountered in this work.

and co-workers[56] in their detailed paper on $C_4H_9^+$ (see their structure no. 10). One might also describe it as an extremely tight π complex of a C_2H_4 unit with a smaller primary carbenium ion, since the three C–C bond distances in the "cyclopropane ring" are roughly 1.4, 1.7, and 1.8 Å. We shall refer to this structure as a primary carbenium ion for simplicity. This minimum was chosen for the carbenium ion to focus only on the initial carbonium dissociation step, since we consider carbenium ion isomerization to be a separate problem beyond the scope of this paper.

Plotted energies correspond to the following reactions:

bond strength (ΔH_{BS}^{298}):

$$C_nH_{2n+2} \rightarrow C_iH_{2i+1} + C_{n-i}H_{2(n-i)+1}$$

proton affinity (ΔH_{PA}^{298}): $\quad C_nH_{2n+3}^+ \rightarrow H^+ + C_nH_{2n+2}$

carbonium dissociation (ΔH_{CD}^{298}):

$$C_nH_{2n+3}^+ \rightarrow C_iH_{2i+1}^+ + C_{n-i}H_{2(n-i)+2}$$

Bronsted-mediated fission (ΔH_{MF}^{298}):

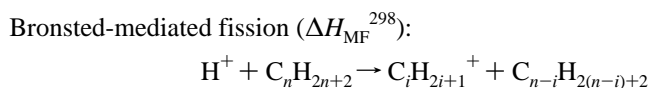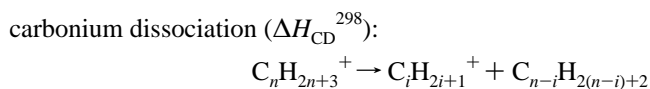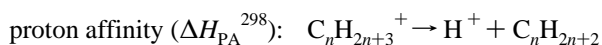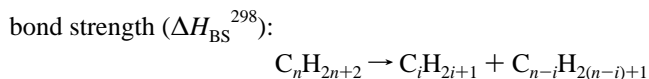$$H^+ + C_nH_{2n+2} \rightarrow C_iH_{2i+1}^+ + C_{n-i}H_{2(n-i)+2}$$

Figure 1 displays these reactions via 3D molecular images, for the case of $n = 10$ and $i = 5$. Note that $\Delta H_{MF}^{298} = \Delta H_{CD}^{298} - \Delta H_{PA}^{298}$; i.e., we use the term Bronsted-mediated fission to represent the sum of the proton attachment and carbonium dissociation steps. These two individual steps of Bronsted-mediated fission are each important in their own right, because they involve carbonium ion thermochemistry while the overall reaction enthalpy does not.

Results

Trends in C–C Bond Strength. Figure 2 plots the bond strength (ΔH_{BS}^{298}) of the central C–C bonds of a series of *n*-alkanes from C_2H_6 to $C_{20}H_{42}$. The theoretical results were computed using B3LYP, MP2, G2, and CCSD(T) levels of theory. The experimental results are derived from values for heats of formation (ΔH_f^{298}) from the National Institute of Standards and Technology;[57] we contrasted the ΔH_f^{298} values for the radical products with those of Berkowicz[58] and Cohen[59]

and found agreement to within 0.5 kcal mol⁻¹. The CCSD(T) results are clearly the best theoretical results, while the other levels of theory are up to 5 kcal mol⁻¹ in error. We did explore the use of the cc-pVTZ basis set to improve the MP2 and B3LYP results (which employed the 6-31G(d,p) basis set; see Theoretical Methods), but this resulted in *worse* results: the MP2 bond strengths rose by 0.6 kcal mol⁻¹, and the B3LYP results fell a surprising 3.5 kcal mol⁻¹.

The CCSD(T) calculations are expensive and could not be performed for the large alkanes, and therefore, the results were extrapolated (dotted line) by taking the B3LYP points for octane and larger and shifting them upward by 5.0 kcal mol⁻¹, this being the difference between the CCSD(T) and B3LYP values for hexane. This extrapolation is expected to be very accurate because the MP2 and B3LYP curves are extremely similar beyond ethane, other than the large constant shift. This extrapolated CCSD(T) curve represents our preferred values for these bond strengths. It agrees with experimental results to within 1 kcal mol⁻¹, except for ethane where the larger disagreement is puzzling and must await further research for its explanation.

Figure 3 plots the bond strength of each C–C bond in $C_{18}H_{38}$ using B3LYP, to compare the bonds within a single alkane. Hence, the leftmost point represents cracking of the alpha C–C bond (the endmost C–C bond), while the rightmost point represents cracking of the central C–C bond (the C–C bond furthest from the ends). The curve is quite similar to the B3LYP curve of Figure 2, and we expect that the CCSD(T) curve in this case should look correspondingly similar to the CCSD(T) curve of Figure 2.

These two figures demonstrate that the C–C bond strength in *n*-alkanes is relatively constant, at about 88 kcal mol⁻¹ at room temperature, except for the terminal (α) and penultimate (β) C–C bonds (89 and 87 kcal mol⁻¹, respectively). Our analysis is apparently the first definitive theoretical demonstration that the weakest C–C bond in an *n*-alkane is the β bond, regardless of alkane length. The explanation of this surprising result awaits further research; at the moment we merely offer the hypothesis that the ethyl radical might have slightly more stability than other primary radicals.

Trends in C–C Proton Affinity. Figure 4 plots the proton affinity (ΔH_{PA}^{298}) of the central C–C bonds of a series of *n*-alkanes, again using B3LYP, MP2, G2, and CCSD(T) theory. The G2 and CCSD(T) values agree to within 1.3 kcal mol⁻¹, and the CCSD(T) result for ethane (142.2 kcal mol⁻¹) is in excellent agreement with experiment (142.7 kcal mol⁻¹).[60] The B3LYP results are particularly poor, being 8–9 kcal mol⁻¹ higher than CCSD(T), although the trend with length of alkane is in agreement with CCSD(T) and MP2. The dotted line indicates the extrapolation of CCSD(T) results by using the B3LYP results as a guide, in the same manner as in Figure 2, to represent the best results.

Figure 5 plots the proton affinity of each C–C bond in $C_{10}H_{22}$ using B3LYP and MP2, to compare the bonds within a single alkane. We expect that the CCSD(T) curve for Figure 5 should be shifted roughly 8–9 kcal mol⁻¹ down from the B3LYP curve, on the basis of the Figure 4 results.

Optimizing the geometry of each protonated alkane was reasonably straightforward, except that protonation of the α bond of $C_{10}H_{22}$ with B3LYP resulted in a monotonically repulsive path to dissociated products rather than a stable carbonium ion. Hence, the B3LYP proton affinity of the α bond that appears in Figure 5 was computed by assuming the dissociated products to be the protonated "supermolecule".
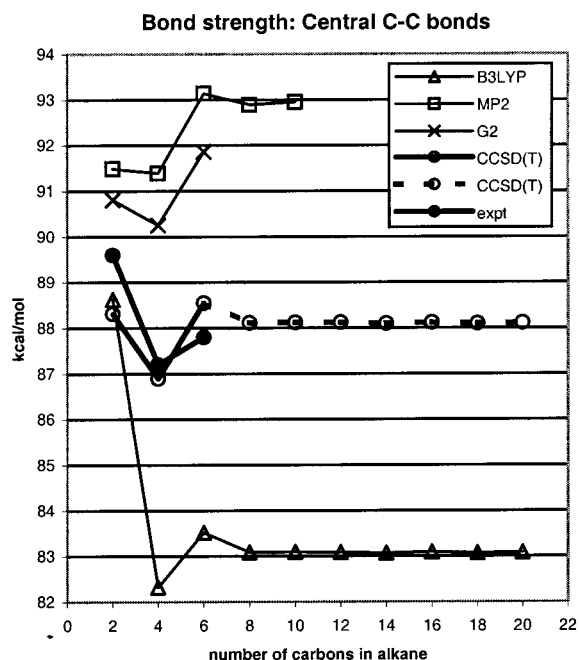
Properties of C−C Bonds in *n*-Alkanes

J. Phys. Chem. A, Vol. 106, No. 7, 2002 **1349**

Figure 2. Bond strengths (ΔH_{BS}^{298}) of the central C−C bonds of *n*-alkanes from C_2H_6 to $C_{20}H_{42}$.

Figure 4. Proton affinities (ΔH_{PA}^{298}) of the central C−C bonds of *n*-alkanes from C_2H_6 to $C_{14}H_{30}$.
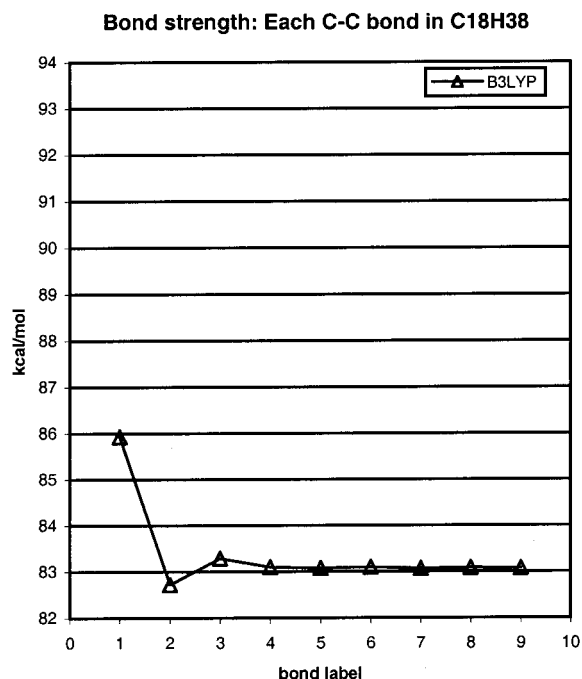

Figure 3. Bond strengths (ΔH_{BS}^{298}) of each C−C bond in $C_{18}H_{38}$ (1 = end C−C bond; 9 = central C−C bond).
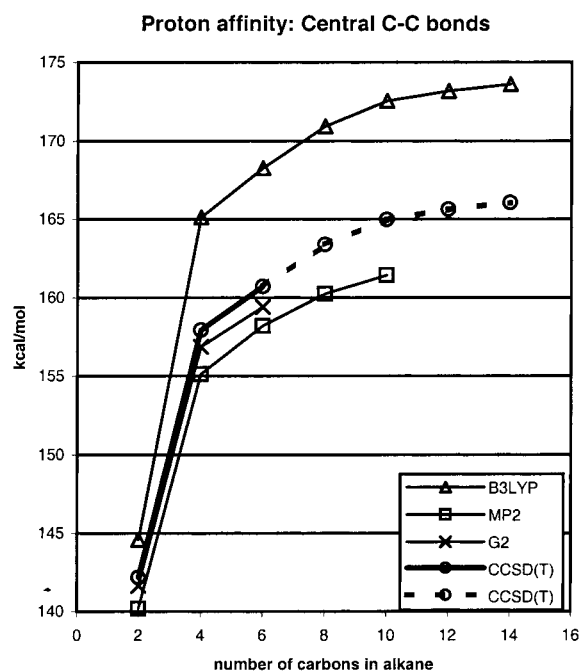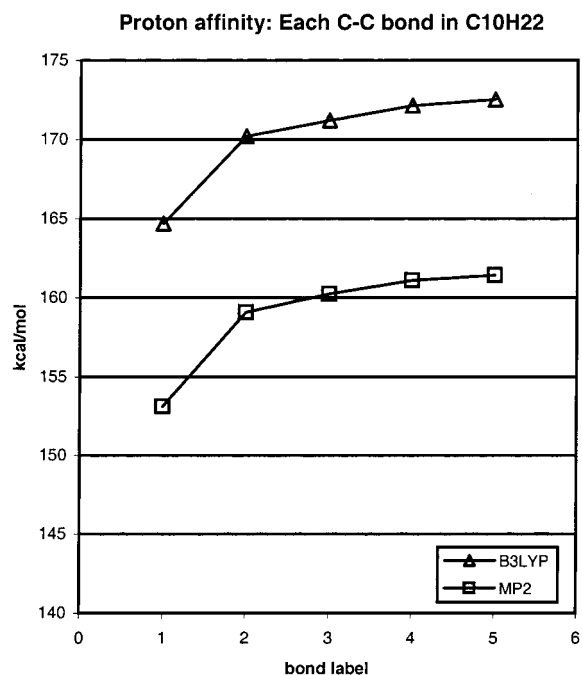

Figure 5. Proton affinities (ΔH_{PA}^{298}) of each C−C bond in $C_{10}H_{22}$ (1 = end C−C bond; 5 = central C−C bond).

The C−C proton affinity is far more sensitive to long-range effects than the C−C bond strength. The results demonstrate that the C−C proton affinity gets monotonically higher for C−C bonds further away from the ends, with the α C−C bond having the least proton affinity.

Trends in Carbonium Dissociation. Figure 6 plots the enthalpy of dissociation (ΔH_{CD}^{298}) of centrally protonated alkanes to a half-sized alkane and half-sized "primary" carbenium ion (see Methods), as a function of the length of the carbon chain, again using B3LYP, MP2, G2, and CCSD(T) theory. The G2 and CCSD(T) results agree to within 0.3 kcal mol^{-1}, with B3LYP and MP2 results in error by up to 2 and 4 kcal mol^{-1}, respectively. The dissociation energy of a protonated alkane is

demonstrated to decrease monotonically with increasing chain length but converging to 7.5 kcal mol^{-1} beyond octonium.

Figure 7 plots these computed dissociation enthalpies for various isomers of protonated decane, $C_{10}H_{23}^{+}$, using B3LYP and MP2. The solid curves represent the preferred dissociation products, which are a short alkane and a long carbenium ion, while the dashed lines represent dissociation to a long alkane and a short carbenium ion. The negative value for the α-protonated decane at the MP2 level indicates that the protonated form is a hanging-well isomer, with a barrier to dissociation. In Figure 7 the trend is rather different from in Figure 6 and indicates that the centrally protonated isomer is actually the isomer requiring the most energy to dissociate, with the
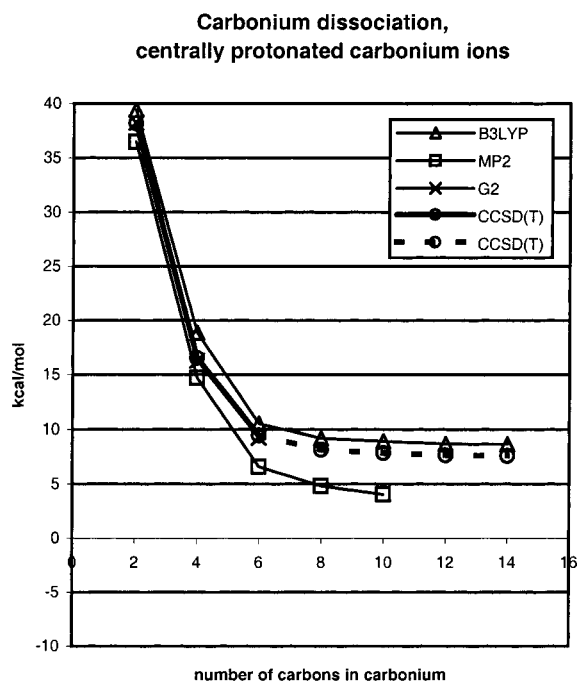
**Carbonium dissociation,
centrally protonated carbonium ions**

Figure 6. Dissociation energies (ΔH_{CD}^{298}) of centrally C−C-protonated carbonium ions from $C_2H_7^+$ to $C_{14}H_{31}^+$. This lowest dissociation channel cracks the C−C bond, producing an alkane and a carbenium ion.
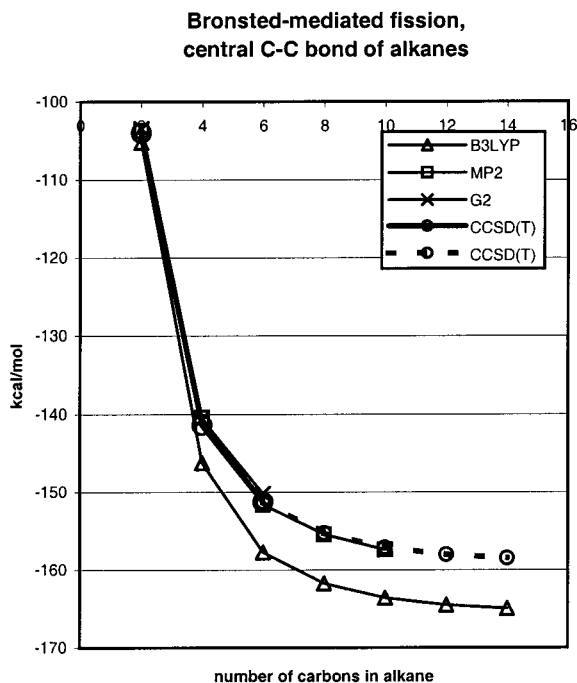
**Bronsted-mediated fission,
central C-C bond of alkanes**

Figure 8. Energies of Bronsted-mediated fission reactions (ΔH_{MF}^{298}) involving the central C−C bonds of *n*-alkanes from C_2H_6 to $C_{14}H_{30}$.

**Carbonium dissociation,
each C-C-protonated isomer of C10H23+**

Figure 7. Dissociation energies (ΔH_{CD}^{298}) of each C−C-protonated isomer of $C_{10}H_{23}^+$ (1 = end C−C bond; 5 = central C−C bond), representing two dissociation channels that both break the C−C bond.

**Bronsted-mediated fission,
each C-C bond of C10H22**

Figure 9. Energies of Bronsted-mediated fission reactions (ΔH_{MF}^{298}) involving each C−C bond in $C_{10}H_{22}$ (1 = end C−C bond; 5 = central C−C bond).

endothermicity falling monotonically as the extra proton is located closer to the end of a carbon chain.

Trends in Bronsted-Mediated Fission. Figure 8 combines the results of Figures 4 and 6 by plotting the net enthalpy of fission (ΔH_{MF}^{298}) of alkanes via central C−C-bond attack by a proton, plotted as a function of the length of the carbon chain. The G2 and MP2 results agree with the CCSD(T) results to within 1.1 kcal mol^{-1}, while B3LYP results are too exothermic by up to 7.5 kcal mol^{-1}. Figure 8 shows that the longer alkanes tend to produce much more exothermic reactions than butane or ethane, with values below −150 kcal mol^{-1}. Remember that
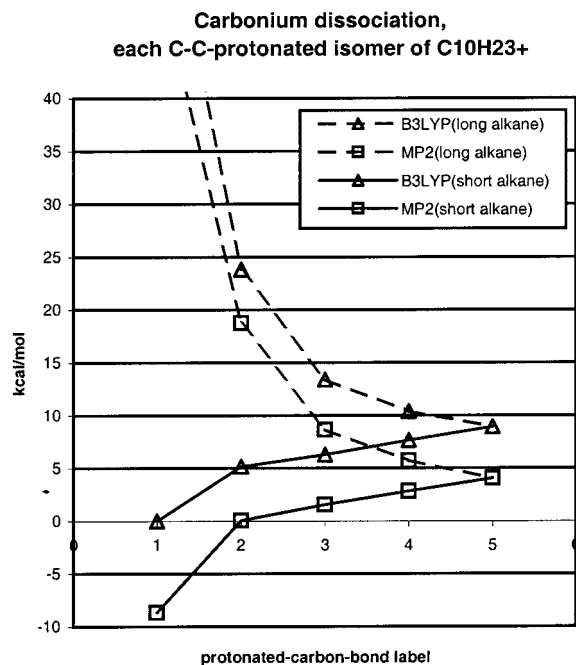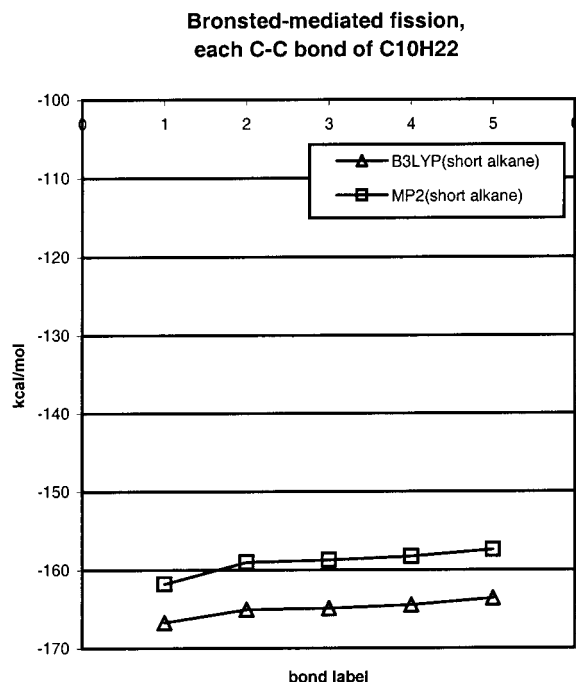
this plot concerns the enthalpy for dissociating only to the "primary" carbenium ion and ignores further net exothermicity from ensuing isomerization or bonding to other species. The trend in this curve is dominated by the trend for proton affinity and enhanced by the trend in carbonium dissociation.

Figure 9 correspondingly combines the results of Figures 5 and 7 by plotting this net enthalpy for the fission of the various C−C bonds of decane. The trend in this curve is dominated by the trend in the carbonium dissociations; i.e., the exothermicity is largest for cracking the bonds toward the end of a long chain.

Properties of C−C Bonds in *n*-Alkanes

J. Phys. Chem. A, Vol. 106, No. 7, 2002 **1351**

TABLE 1: Best Values for Enthalpies of Reaction (ΔH²⁹⁸, 1 atm Pressure) Involving the Central C−C Bonds of All-Trans *n*-Alkanes, Based on CCSD(T)/cc-pVTZ Calculations with Corrections and Extrapolations[a]

alkane length	bond strength	proton affinity	carbonium dissn	mediated fission
C_2	88.3	142.2	38.2	−104.0
C_4	86.9	157.9	16.5	−141.4
C_6	88.5	160.7	9.4	−151.3
C_8	88.1	163.4	8.1	−155.3
C_{10}	88.1	165.0	7.8	−157.1
C_{12}	88.1	165.6	7.6	−158.0
C_{14}	88.1	166.1	7.6	−158.5

[a] See text.

TABLE 2: Temperature Corrections (ΔH²⁹⁸ − ΔE°) for Reaction Enthalpies, from B3LYP/6-31G(d,p) Calculations

alkane length	bond strength	proton affinity	carbonium dissn	mediated fission
C_2	2.3	0.8	+1.3	+0.5
C_4	1.9	0.5	+0.2	−0.3
C_6	1.6	0.5	−0.0	−0.5
C_8	1.4	0.5	−0.2	−0.7
C_{10}	1.3 (1.2)[a]	0.5 (0.8)[a]	−0.3 (−0.2)[a]	−0.8 (−0.9)[a]

[a] Value is from MP2/6-31G(d,p) calculations, for comparison.

TABLE 3: Zero-point Vibrational Energy Corrections (ΔE° − ΔE_raw) for Reaction Enthalpies, from B3LYP/6-31G(d,p) Calculations

alkane length	bond strength	proton affinity	carbonium dissn	mediated fission
C_2	−9.7	−5.0	−4.1	0.9
C_4	−8.4	−3.3	−1.2	2.1
C_6	−7.6	−3.7	−0.1	3.6
C_8	−7.4	−3.6	+0.2	3.8
C_{10}	−7.3 (−7.1)[a]	−3.6 (−5.2)[a]	+0.3 (−1.0)[a]	3.9 (4.2)[a]

[a] Value is from MP2/6-31G(d,p) calculations, for comparison.

Trends in the Corrections for ZPVE and Temperature. Table 1 lists our best values for the four reaction enthalpies involving the central C−C bonds of all-trans *n*-alkanes. These are the CCSD(T)-based values from Figures 2, 4, 6, and 8. These ΔH²⁹⁸ reaction enthalpies are computed by adding two corrections to the raw electronic energy differences. The first is due to zero-point vibrational energies (ZPVE), computed here for each molecule as half the sum of its unscaled B3LYP harmonic vibrational frequencies. The second is due to temperature, computed from usual statistical formulas using the rigid-rotor/harmonic oscillator approximation, together with B3LYP data. The magnitude of these corrections for reaction energies is very consistent for reactions involving more than 4 carbons. Table 2 lists the temperature corrections, for those who may be interested in converting our data to zero-Kelvin results for instance. Table 3 lists the ZPVE corrections. In Tables 2 and 3 we include a comparison to MP2/6-31G(d,p) results for 10-carbon systems, and we see that the agreement with B3LYP results is very good (within 0.3 kcal mol⁻¹) except for the reactions involving carbonium ions, where the difference in zero-point energies among methods is over 1 kcal mol⁻¹. This is due to the disagreement over the nature of the 3-center−2-electron bond, which is loose according to B3LYP but stiffer according to MP2. If the MP2 corrections turn out to be more accurate, then our best proton affinities (listed in Table 1) would be lowered by roughly 1.3 kcal mol⁻¹ for butane and longer alkanes.

Trends in Geometrical Parameters. Figure 10 plots MP2/6-31G(d,p) data for the C−C bond lengths of C_9H_{20}, the C_9H_{19}

C-C bond lengths: Comparing C9H20, primary radical C9H19 and primary carbenium C9H19+
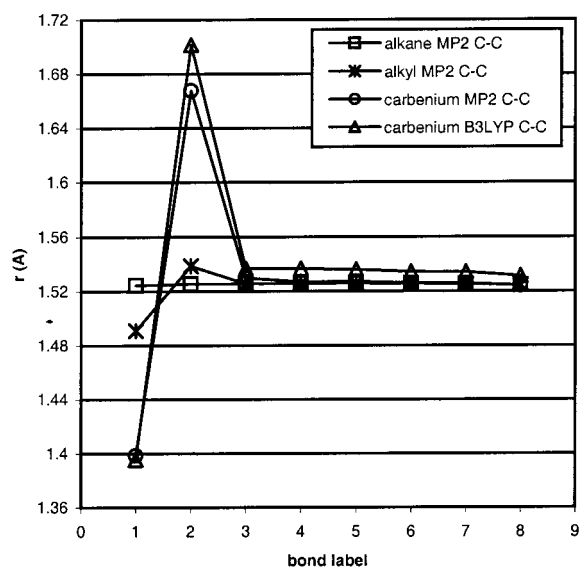
Figure 10. Optimized C−C bond lengths (Å). Bond 1 is the C−C bond nearest the active end (α), while bond 8 is the C−C bond at the other end of the molecule. For C_9H_{20}, both these bonds are equivalent.

radical, and the $C_9H_{19}^+$ carbenium ion, with the numbering of the bonds (1, 2, 3, ... or α, β, γ, ...) starting from the active end of the molecule. The alkane bond lengths are fairly constant at 1.526 Å, with slightly smaller α bonds. The bond lengths of the radical are nearly identical except for the β bond (0.013 Å larger) and the α bond (0.035 Å smaller). The bond lengths of the carbenium ions are more interesting, with the deviations from the constant value being +0.004, +0.142, −0.127 Å for the γ, β, and α bonds, respectively. The reason for these particularly unusual β and α bond lengths is the preference of long primary carbenium ions to stabilize the charge by forming the "protonated cyclopropane" structure (see Methods), with a short α bond and an elongated β bond. The B3LYP/6-31G-(d,p) bond lengths are uniformly 0.008 Å longer than the MP2 results, except for the carbenium ion results, so we added these to Figure 10 for comparison.

Next we looked at the dependence of some of these bond lengths upon molecular chain length. Table 4 presents the MP2/6-31G(d,p) data for the α, β, and γ bonds of the alkanes, alkyl radicals, and carbenium ions. The short α bond is seen to be even shorter for the small alkanes but on a very small scale. The long β bond of the carbenium ions is particularly long for propenium, simply due to the γ carbon being part of a CH_3^+ unit which is somewhat equally drawn to the α carbon as to the β carbon.

Figure 11 is equivalent to Figure 10 except that it concerns the C−H bond lengths. For the alkanes and alkyl radicals, Figure 11 concerns only the bonds to H atoms above and below the carbon atom plane of symmetry. For alkanes, these CH bond lengths are fairly constant at 1.094 Å, except on the β and α carbons where they are up to 0.004 Å smaller. On the radical molecule, the CH bonds on the radical carbon are 0.015 Å smaller than normal. For the C_1-symmetry carbenium ions, there are two MP2 curves in the figure because the α carbon (on the C_2H_4 unit) is twisted 60° out-of-plane around the β bond, creating a difference between the C−H bonds on either side of the usual carbon atom plane. The carbenium C−H bonds on

TABLE 4: Optimized α-, β-, and γ-C−C-Bond Lengths (Å) of *n*-Alkanes, Primary Radicals, and "Primary" Carbenium Ions, According to MP2/6-31G(d,p), and Displayed with Increasing Carbon Chain Length from Left to Right

C−C bond	C_2	C_3	C_4	C_5	C_6	C_7	C_8	C_9
alkane α	1.5234	1.5241	1.5243	1.5245	1.5246	1.5246	1.5246	1.5246
alkane β	n/a	n/a	1.5252	1.5253	1.5256	1.5256	1.5256	1.5256
alkane γ	n/a	n/a	n/a	n/a	1.5254	1.5256	1.5257	1.5257
alkyl α	1.4890	1.4914	1.4907	1.4909	1.4909	1.4909	1.4909	1.4909
alkyl β	n/a	1.5362	1.5382	1.5383	1.5387	1.5387	1.5387	1.5387
alkyl γ	n/a	n/a	1.5243	1.5255	1.5255	1.5258	1.5258	1.5258
carbenium α	1.3828	1.3941	1.3816	1.3842	1.3846	1.3846	1.3847	1.3848
carbenium β	n/a	1.7909	1.7417	1.7228	1.7222	1.7217	1.7210	1.7207
carbenium γ	n/a	n/a	1.5567	1.5721	1.5721	1.5728	1.5734	1.5736
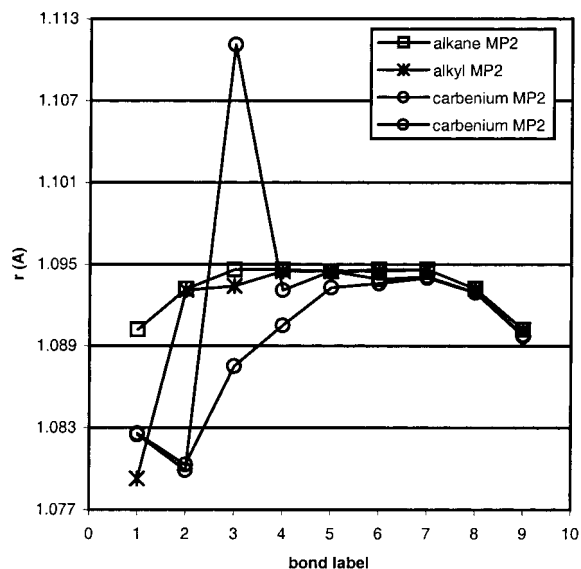
Figure 11. Optimized C−H bond lengths (Å) for the hydrogen atoms above and below the plane of the carbon atom chain. Bond 1 denotes the C−H bonds of the α-carbon, while bond 9 denotes the C−H bonds of the carbon at the other end of the molecule. For $C_9H_{19}^+$, these C−H bonds at each carbon are not equivalent, and so two curves are presented for this ion.

the α and β carbons (bonds 1 and 2, respectively) are short (1.080−1.083 Å) because they are part of the C_2H_4 unit. The great discrepancy between the C−H bonds on the 3rd carbon (1.088 and 1.111 Å) is due to the effects of the C_2H_4 unit, whose C−C bond eclipses one of these C−H bonds and makes it rather long.

Next we examined the geometrical structure aspects of the carbenium ions. For the CHC 3-center−2-electron bond, the B3LYP and MP2 results differed dramatically and, hence, are both presented. Figure 12 plots the angle θ_{CHC} of the 3-center−2-electron bond in centrally protonated *n*-alkanes, as a function of chain length, and here we see that the MP2 angle is generally near 130°, while the B3LYP angle is generally above 150° and approaches linearity (above 170°) for carboniums having 10 carbons or more. Figure 13 plots the corresponding changes in the distance R_{CC}, and here the MP2 calculations predict 2.2 Å while the B3LYP calculations predict 2.5 Å, entirely concomitant with the disagreement in the C−H−C angle. The trends of θ_{CHC} and R_{CC} as a function of protonation position on a decane chain can be seen in the data displayed in Table 5. The trends with chain length and location on chain suggest that θ_{CHC} and R_{CC} both get larger with increasing proton affinity of the original C−C bond; i.e., the greater the proton affinity, the closer the proton can tuck into the absolute center of the C−C bond
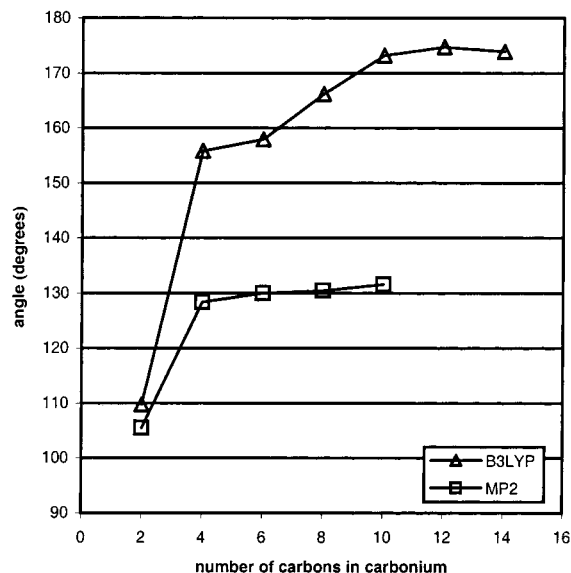
Figure 12. Optimized CHC angles for the 3-center−2-electron bond in centrally σ_{C-C}-protonated carbonium ions from $C_2H_7^+$ to $C_{14}H_{31}^+$.

density. We suspect, on the basis of the results for proton affinity, that the true gas-phase geometrical structures of these carboniums likely lie closer to the MP2 results than the B3LYP ones; i.e., a CHC angle of 135−150° and a C−C bond length of 2.3−2.4 Å.

Trends in Vibrational Frequencies. With regard to the computed vibrational frequencies and the infrared (IR) intensities, the result we would like to stress the most is the following: free carbonium ions, if they live long enough in solution, can be clearly identified using IR spectroscopy due to a very intense peak, in the 2100−2300 cm⁻¹ range if gaseous and shifted to lower wavenumbers in condensed phases. We examined the predicted IR gas-phase spectra of several compounds using B3LYP and MP2 levels of theory and can provide a rough summary of the spectra here.

Let the intensity of the allowed C−H stretch modes in the 3000−3100 range be considered to have magnitude of $I = 1$. Then the following holds: (i) The all-trans alkanes will have no other IR peaks as bright as these. (ii) The primary radicals have a peak at around 530 cm⁻¹ having $I = 1$ for *n*-butyl, which gets weaker for the longer *n*-alkyl radicals; this absorption is due to the inversion mode at the radical carbon center. (iii) The unstable primary carbenium ions show several $I = 1$ peaks other than C−H stretches, in the ranges 300−400, 1000−1100, and 1300−1500 cm⁻¹. (iv) The centrally σ_{C-C}-protonated carbonium ions, however, produce three *massive* peaks near 2150 cm⁻¹ (with $I > 100$), 850 cm⁻¹ (with $I > 50$), and 1110

Properties of C−C Bonds in *n*-Alkanes

J. Phys. Chem. A, Vol. 106, No. 7, 2002 **1353**

TABLE 5: CHC 3-Center−2-Electron Bond of Deconium Ion: Variation of Geometrical Parameters with Choice of σ_{C-C} Bond for Protonation

parameter	1 (C_α–C_β)	2 (C_β–C_γ)	3 (C_γ–C_δ)	4 (C_δ–C_ϵ)	5 (C_ϵ–C_ϵ)
θ_{CHC} (deg), B3LYP	dissociated	168.4	168.2	176.7	173.2
θ_{CHC} (deg), MP2	124.2	130.3	130.6	131.3	131.6
R_{CC} (Å), B3LYP	dissociated	2.531	2.526	2.538	2.534
R_{CC} (Å), MP2	2.197	2.243	2.245	2.252	2.255
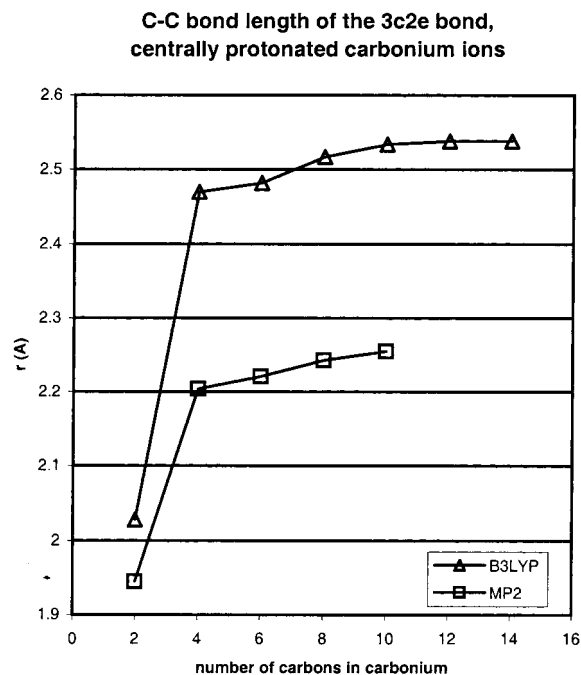
Figure 13. Optimized C−C bond lengths (Å) for the 3-center−2-electron bond in centrally σ_{C-C}-protonated carbonium ions from $C_2H_7^+$ to $C_{14}H_{31}^+$.

Figure 14. Bubble plot of the most intense infrared bands of centrally σ_{C-C}-protonated carbonium ions from $C_4H_{11}^+$ to $C_{14}H_{31}^+$. The size of the points is proportional to the computed absolute intensities (km mol^{-1}) of the bands. The 2150 cm^{-1} band should be a signature band that can be used to identify the presence of free carbonium ions.
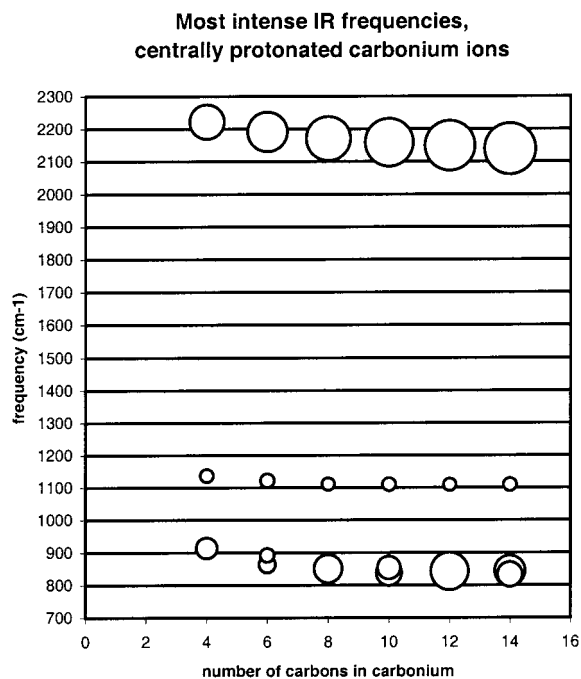
cm^{-1} (with $I > 20$), due to modes involving motion of the bridging proton.

Figure 14 plots the unscaled B3LYP harmonic frequencies of the three brightest modes of these centrally protonated carboniums, as a function of length of the carbon chain, to display the subtle effects of chain length upon peak position. The size of the points indicates the relative IR intensity of the peaks. Note that the absorption band near 850 cm^{-1} is actually two overlapping bands for the C_6, C_{10}, and C_{14} carboniums.

We also examined the intense carbonium absorption frequency for protonated decane as a function of protonation position on the chain (α, β, γ, δ, and ϵ bonds), but the results appear fairly constant, within a 15 cm^{-1} range, except for the hypothetical α-protonated isomer. Hence it would be difficult to use this mode to identify which C−C site has been protonated in an experiment.

Besides the C−C-protonated carbonium ions, the only other hydrocarbon species we could fathom which might give a peak near 2200 cm^{-1} would be *carbenium* ions with a bridging proton, such as $C_2H_5^+$ or $(CH_3)_2CHC(CH_3)_2^+$. However, the B3LYP results for $C_2H_5^+$ place the same along-the-bond mode at a much lower frequency (540 cm^{-1}), and although a perpendicular motion of the bridging proton does give a frequency near 2200 cm^{-1}, it has a much lower intensity ($I = 3$) than the carbonium ion ($I > 100$).

While checking some of the animations of the computed harmonic-frequency normal modes, we observed a set of alkane chain-bending frequencies that had the appearance of classical normal modes of a vibrating spring. We sorted the B3LYP vibrational frequencies of $C_{20}H_{42}$ and collected the set of "string

modes" for in-plane bending and another set for out-of-plane bending (where the plane is the carbon atom plane). This was not always simple, due to vibrational coupling, but was fairly straightforward for the first 7 harmonic frequencies of each set. The B3LYP frequencies are shown in Figure 15, as a function of the string mode index n. We fit these data very well with the following formulas: $\nu_n = 11.1n^{1.656}$ for in-plane string modes; $\nu_n = 8.0n^{1.536}$ for out-of-plane string modes. We remind the reader of the known results for the frequencies for a classical string fixed at both ends (vary with n^1) and frequencies for a quantum particle-in-a-box (vary with n^2). Results for polyalkyne chains in our laboratory[61] suggest that the observed powers of n will tend toward 2 if the chain is infinitely lengthened and if the ends are made infinitely heavy.

Discussion

The curious implication, based on radical heats of formation, that the β C−C bond is the weakest C−C bond in *n*-hexane[3] has been demonstrated with CCSD(T) computations to not only be correct but to be a common feature of *n*-alkanes. The B3LYP and MP2 calculations were not sufficient to demonstrate this, due to their 5 kcal mol^{-1} inaccuracy which prevents them from discerning between the 1 kcal mol^{-1} variations. Therefore, we expect an enhancement of ethyl radicals over other radicals in the initial activation step in pyrolysis of *n*-alkanes.

We have demonstrated that the proton affinity of C−C bonds between secondary substituted carbons is a more sensitive
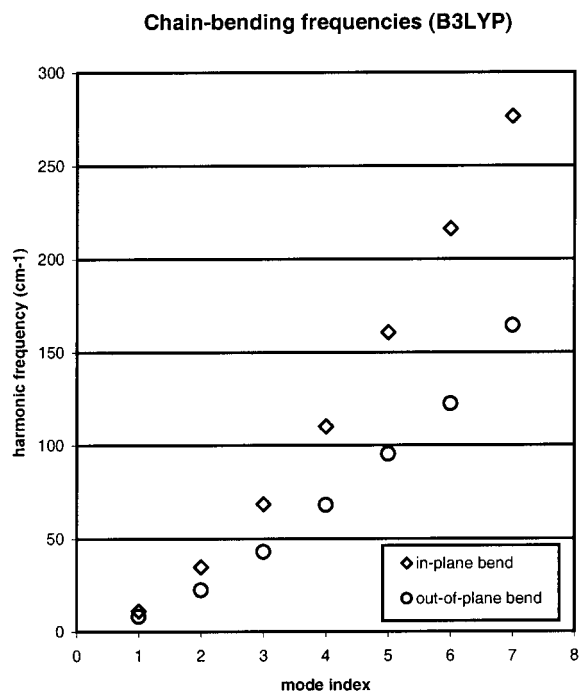
Chain-bending frequencies (B3LYP)

Figure 15. Computed B3LYP/6-31G(d,p) harmonic frequencies for chain-bending or "string modes" of all-trans $C_{20}H_{42}$. The mode index n indicates that the mode has $n - 1$ nodes in the middle of the "string."

Summary of C–C-bond proton affinities

Figure 16. Summary of CCSD(T) and extrapolated values of proton affinities (ΔH_{PA}^{298}) of all the C–C bonds of even-length all-trans n-alkanes up to decane. Most results arise from corrections to B3LYP results, as justified by Figures 2–9.

quantity to long-range effects than the C–C bond strength is. For all-trans n-alkanes, these proton affinites vary from 142 kcal mol^{-1} (for ethane) to over 166 kcal mol^{-1}, with no apparent convergence of value even after 7 carbons are placed on either side of the target bond.

The lowest energy dissociation asymptote for a σ_{C-C}-protonated alkane is the fission of the C–C bond. Our results demonstrate that this dissociation prefers to make the shorter fragment an alkane and the larger fragment a carbenium ion, with the ion appearing (at least initially) rather like a protonated alkylcyclopropane. The results also indicate that an n-carbonium ion protonated at the α C–C-bond position may dissociate without bound if the original alkane is long enough (perhaps for n-butane and longer).

Figure 8, the plot of exothermicity for Bronsted-mediated fission of central C–C bonds in n-alkanes strongly suggests that longer alkanes are more susceptible to this kind of fission than shorter ones. This trend arises from the trends of the two components to this enthalpy, namely the proton affinity (Figure 4) and carbonium dissociation energy (Figure 6). In a condensed-phase system, the exothermicity will be greatly reduced because the original "H$^+$" unit will have its initial energy lowered by solvation, and for many catalytic systems this would likely cause this fission process to be endothermic for the smallest alkanes. There is a smaller but also significant solvation effect for the product carbenium ion, particularly in cases where it bonds covalently to a catalyst.

Figure 9 gave an unexpected result. It suggests that the most thermodynamically favored places for Bronsted fission of an n-alkane are not the bonds of greatest proton affinity (the central bonds) but the bonds nearest the end of the alkane chain. This implies that the direct cracking, via proton transfer from a Bronsted acid, of an α C–C bond in an n-alkane has the greatest exothermicity (compared to the other C–C bonds) despite apparently having the highest activation energy. This would result in the conclusion that a half-sized alkane is the pre-
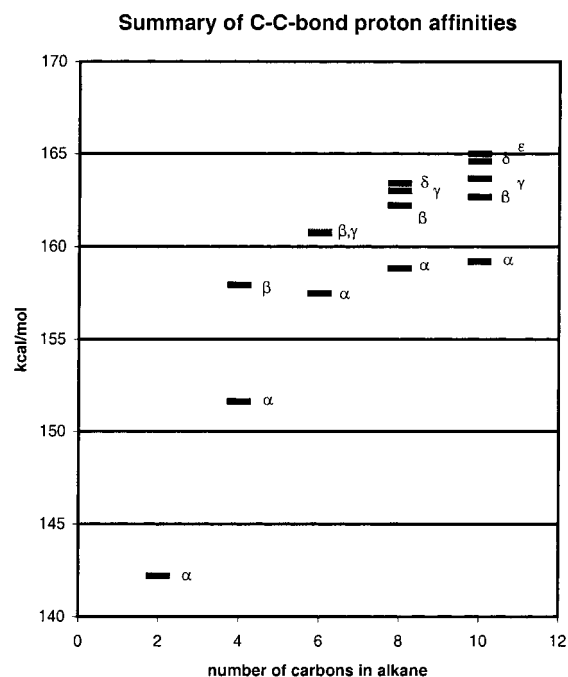
ferred alkane product kinetically but that methane is the preferred alkane product thermodynamically. We offer two comments. First, the relevance to condensed phases is rather limited because "solvent effects" or "catalytic effects" are likely to swamp the small (2 kcal mol^{-1}) variations in net mediated fission exothermicity. Second, we suspect that the two steps of proton donation to the alkane and ensuing dissociation of the carbonium ion are sufficiently "nonconcerted" as to kinetically allow vibrational and even geometrical rearrangement of the carbonium intermediate, including various σ_{C-C} and σ_{C-H} isomers, before dissociation occurs. This is certainly the case with the reaction $H_2 + C_2H_5^+ \leftrightarrow CH_4 + CH_3^+$ in the gas phase, a case with which we are more familiar.[37] Although a 1996 paper by Blaszkowski et al.[28] suggested that Bronsted-mediated fission of ethane over zeolite is a concerted one-step reaction, later work by Zygmunt et al.[33,34] shows less straightforward atomic motions. Our group is currently investigating this matter.

We like to imagine the reactivity of alkanes in strong liquid or solid Bronsted acids as an act of tug-of-war, as the activated H$^+$ ion is weakly attracted to both the alkane and the very weak conjugate base of the acid. When viewed in this way, the protons would only be likely to activate or crack the alkane in this proposed manner if the alkane has a site of greater proton affinity than the original site on the catalyst. Taking results from Figures 4 and 5 and other data of ours, we created a new figure, Figure 16, which summarizes our best set of results for the proton affinities of all C–C bonds in several n-alkanes. This figure could explain why a particular Bronsted catalyst might crack n-octane but not n-hexane, by arguing that the catalyst in this case has a conjugate base site with an effective (gas-phase) proton affinity near 163 kcal mol^{-1}. Solvent effects should shift the values in Figure 16 by a somewhat constant amount in most cases.

On the technical side, we stress that carbonium ions are more difficult to compute accurately than carbenium ions and alkanes.

Properties of C−C Bonds in *n*-Alkanes

J. Phys. Chem. A, Vol. 106, No. 7, 2002 **1355**

This is because of the 3-center−2-electron bonds, which appear to be a challenge for electron correlation methods. The MP2/6-31G(d,p) results for Bronsted-mediated fission, whose computed energy does not involve carbonium ions, agree with CCSD(T) results to within 1 kcal mol^{-1}, but the energies for the half-reactions (formation of carbonium, and ensuing dissociation) are in error by up to 4 kcal mol^{-1} due to such difficulties. The B3LYP/6-31G(d,p) results happen to be accurate (within 2 kcal mol^{-1}) for our carbonium ion dissociations, but this is perhaps a fortunate cancellation of errors since its results are up to 7.5 kcal mol^{-1} too low for the more straightforward Bronsted-mediated fission energies and up to 9 kcal mol^{-1} too high for proton affinities. In particular, we have concerns regarding reported claims[62] that density functional theory is giving appropriate energetics for carbonium calculations, and we remind readers that great care must be exercised in making interpretations based on such studies.

Summary

Our CCSD(T) calculations demonstrate, for the first time computationally, that the β C−C bond is the weakest C−C bond in an *n*-alkane, with a bond strength roughly 1 kcal mol^{-1} less than the usual *n*-alkane value (ΔH^{298}) of 88 kcal mol^{-1}. The B3LYP and MP2 calculations were not sufficient to demonstrate this, due to their 5 kcal mol^{-1} inaccuracy which prevents them from discerning between the 1 kcal mol^{-1} variations. This result suggests a slight enhancement of ethyl radicals over other radicals in the initial activation step in the pyrolysis of *n*-alkanes.

We have demonstrated that the proton affinity of C−C bonds between secondary substituted carbons is a more sensitive quantity to long-range effects than the C−C bond strength is. For all-trans *n*-alkanes, the proton affinities (ΔH^{298}) vary from 142 kcal mol^{-1} (for ethane) to over 166 kcal mol^{-1} and increase monotonically from the end of the alkane chain to the center. Hence, in a sample of mixed straight-chain alkanes, the C−C bond with the highest proton affinity should be the central C−C bond of the longest alkane.

Computations of carbonium dissociation and Bronsted-mediated fission demonstrate that long alkanes are more susceptible to this kind of C−C bond fission than smaller alkanes. However, within an alkane, Bronsted-mediated fission of the end C−C bonds, rather than the central C−C bonds, produces slightly more exothermicity in the gas phase. End fission via acid catalysts may require more activation energy however, both in condensed and gas phases.

Limitations in accuracy of the B3LYP and MP2 methods are demonstrated and quantified here when used in conjunction with the 6-31G(d,p) basis set. Greatest discrepancies are seen in computations involving carbonium ions, due to the 3-center−2-electron bonds.

Carbonium ions with a CCH 3-center−2-electron bond are predicted to have a very intense and characteristic IR band, in the 2100−2300 cm^{-1} region for gaseous ions and a somewhat red-shifted region for condensed-phase ions. This should constitute a signature IR band which could prove vital in the search for these elusive ions.

References and Notes

(1) Wojciechowski, B. W.; Corma, A. *Catalytic Cracking: Catalysts, Chemistry, and Kinetics*; Dekker: New York, 1986.

(2) Olah, G. A.; Molnar, A. *Hydrocarbon Chemistry*; Wiley: New York, 1995.

(3) Imbert, F. E.; Marshall, R. M. *Int. J. Chem. Kinet.* **1987**, *19*, 81.

(4) Brouwer, D. M.; Hogeveen, H. *Prog. Phys. Org. Chem.* **1972**, *9*, 179.

(5) Scherzer, J. *Catal. Rev.−Sci. Eng.* **1989**, *31*, 215.

(6) Culmann, J.-C.; Sommer, J. *J. Am. Chem. Soc.* **1990**, *112*, 4057.

(7) Fǎrcaşiu, D. *Catal. Lett.* **2001**, *71*, 95.

(8) Adeeva, V.; Liu, H.-Y.; Xu, B.-Q.; Sachtler, W. M. H. *Top. Catal.* **1998**, *6*, 61.

(9) Olah, G. A.; Halpern, Y.; Shen, J.; Mo, Y. K. *J. Am. Chem. Soc.* **1973**, *95*, 4960.

(10) Haag, W. O.; Dessau, R. M. *Proc. Int. Congr. Catal., 8th* **1985**, *2*, 305.

(11) Sommer, J.; Bukula, J.; Hachoumy, M.; Jost, R. *J. Am. Chem. Soc.* **1997**, *119*, 3274.

(12) Ivanova, I. I.; Pomakhina, E. B.; Rebrov, A. I.; Derouane, E. G. *Top. Catal.* **1998**, *6*, 49.

(13) Brenner, A. M.; Schrodt, J. T.; Shi, B.; Davis, B. H. *Catal. Today* **1998**, *44*, 235.

(14) Goeppert, A.; Sassi, A.; Sommer, J.; Esteves, P. M.; Mota, C. J. A.; Karlsson, A.; Ahlberg, P. *J. Am. Chem. Soc.* **1999**, *121*, 10628.

(15) Williams, B. A.; Ji, W.; Miller, J. T.; Snurr, R. Q.; Kung, H. H. *Appl. Catal., A* **2000**, *203*, 179.

(16) Demeyer, A.; Ceulemans, J. *J. Phys. Chem. A* **2000**, *104*, 4004.

(17) Ahlberg, P.; Karlsson, A.; Goeppert, A.; Nilsson Lill, S. O.; Dinér, P.; Sommer, J. *Chem. Eur. J.* **2001**, *7*, 1936.

(18) Boronat, M.; Viruela, P.; Corma, A. *J. Phys. Chem. B* **1997**, *101*, 10069.

(19) Boronat, M.; Viruela, P.; Corma, A. *J. Phys. Chem. A* **1998**, *102*, 9863.

(20) Boronat, M.; Viruela, P.; Corma, A. *J. Phys. Chem. B* **1999**, *103*, 7809.

(21) Boronat, M.; Viruela, P.; Corma, A. *Phys. Chem. Chem. Phys.* **2000**, *2*, 3327.

(22) Mota, C. J. A.; Esteves, P. M.; Ramírez-Solís, A.; Hernández-Lamoneda, R. *J. Am. Chem. Soc.* **1997**, *119*, 5193.

(23) Esteves, P. M.; Mota, C. J. A.; Ramírez-Solís, A.; Hernández-Lamoneda, R. *Top. Catal.* **1998**, *6*, 163.

(24) Esteves, P. M.; Nascimento, M. A. C.; Mota, C. J. A. *J. Phys. Chem. B* **1999**, *103*, 10417.

(25) Esteves, P. M.; Alberto, G. G. P.; Ramírez-Solís, A.; Mota, C. J. A. *J. Am. Chem. Soc.* **1999**, *121*, 7345.

(26) Esteves, P. M.; Ramírez-Solís, A.; Mota, C. J. A. *J. Braz. Chem. Soc.* **2000**, *11*, 345.

(27) Esteves, P. M.; Ramírez-Solís, A.; Mota, C. J. A. *J. Phys. Chem. B* **2001**, *105*, 4331.

(28) Blaszkowski, S. R.; Nascimento, M. A. C.; van Santen, R. A. *J. Phys. Chem.* **1996**, *100*, 3463.

(29) Frash, M. V.; Solkan, V. N.; Kazansky, V. B. *J. Chem. Soc., Faraday Trans.* **1997**, *93*, 515.

(30) Frash, M. V.; van Santen, R. A. *Top. Catal.* **1999**, *9*, 191.

(31) Kazansky, V. B. *Catal. Today* **1999**, *51*, 419.

(32) Chatterjee, A.; Iwasaki, T.; Ebina, T.; Tsuruya, H.; Kanougi, T.; Oumi, Y.; Kubo, M.; Miyamoto, A. *Proc. Int. Zeolite Conf., 12th* **1999**, *1*, 489.

(33) Zygmunt, S. A.; Curtiss, L. A.; Iton, L. E. *Proc. Int. Zeolite Conf., 12th* **1999**, *1*, 333.

(34) Zygmunt, S. A.; Curtiss, L. A.; Zapol, P.; Iton, L. E. *J. Phys. Chem. B* **2000**, *104*, 1944.

(35) Bates, S. P.; van Santen, R. A. *Adv. Catal.* **1998**, *42*, 1.

(36) Tal'roze, V. L.; Lyubimova, A. L. *Dokl. Akad. Nauk SSSR* **1952**, *86*, 909; *Chem. Abstr.* **1953**, *47*, 2590.

(37) East, A. L. L.; Liu, Z. F.; McCague, C.; Cheng, K.; Tse, J. S. *J. Phys. Chem. A* **1998**, *102*, 10903.

(38) Esteves, P. M.; Mota, C. J. A.; Ramírez-Solís, A.; Hernandez-Lamoneda, R. *J. Am. Chem. Soc.* **1998**, *120*, 3213.

(39) Esteves, P. M.; Alberto, G. G. P.; Ramírez-Solís, A.; Mota, C. J. A. *J. Phys. Chem. A* **2000**, *104*, 6233.

(40) Corma, A.; Planelles, J.; Sánchez-Marín, J.; Tomás, F. *J. Catal.* **1985**, *93*, 30.

(41) Corma, A.; Planelles, J.; Tomás, F. *J. Catal.* **1985**, *94*, 445.

(42) Otto, A. H.; Prescher, D.; Gey, E.; Schrader, S. *J. Fluor. Chem.* **1997**, *82*, 55.

(43) Collins, S. J.; O'Malley, P. J. *Top. Catal.* **1998**, *6*, 151.

(44) Hall, W. K.; Lombardo, E. A.; Engelhardt, J. *J. Catal.* **1989**, *115*, 611.

(45) Kotrel, S.; Knozinger, H.; Gates, B. C. *Microporous Mesoporous Mater.* **2000**, *35*, 11.

(46) Frisch, M. J.; Trucks, G. W.; Schlegel, H. B.; Scuseria, G. E.; Robb, M. A.; Cheeseman, J. R.; Zakrzewski, V. G.; Montgomery, J. A.; Stratmann, R. E.; Burant, J. C.; Dapprich, S.; Millam, J. M.; Daniels, A. D.; Kudin, K. N.; Strain, M. C.; Farkas, O.; Tomasi, J.; Barone, V.; Cossi, M.; Cammi, R.; Mennucci, B.; Pomelli, C.; Adamo, C.; Clifford, S.; Ochterski, J.; Petersson, G. A.; Ayala, P. Y.; Cui, Q.; Morokuma, K.; Malick, D. K.; Rabuck, A. D.; Raghavachari, K.; Foresman, J. B.; Cioslowski, J.; Ortiz, J. V.; Stefanov, B. B.; Liu, G.; Liashenko, A.; Piskorz, P.; Komaromi, I.; Gomperts, R.; Martin, R. L.; Fox, D. J.; Keith, T.; Al-Laham, M. A.; Peng, C. Y.; Nanayakkara, A.; Gonzalez, C.; Challacombe, M.; Gill, P. M. W.; Johnson, B. G.; Chen, W.; Wong, M. W.; Andres, J. L.; Head-Gordon, M.; Replogle, E. S.; Pople, J. A. *Gaussian 98*, revision A.9; Gaussian, Inc.: Pittsburgh, PA, 1998.

(47) McQuarrie, D. A. *Statistical Mechanics*; Harper & Row: New York, 1976.

(48) Becke, A. D. *J. Chem. Phys.* **1993**, *98*, 5648.

(49) Lee, C.; Yang, W.; Parr, R. G. *Phys. Rev. B* **1988**, *37*, 785.

(50) Møller, C.; Plesset, M. S. *Phys. Rev.* **1934**, *46*, 618.

(51) Curtiss, L. A.; Raghavachari, K.; Trucks, G. W.; Pople, J. A. *J. Chem. Phys.* **1991**, *94*, 7221.

(52) Cizek. J. *Adv. Chem. Phys.* **1969**, *14*, 35.

(53) Pople, J. A.; Head-Gordon, M.; Raghavachari, K. *J. Chem. Phys.* **1987**, *87*, 5968.

(54) Bartlett, R. J. *J. Phys. Chem.* **1989**, *93*, 1697.

(55) Dunning Jr., T. H. *J. Chem. Phys.* **1989**, *90*, 1007.

(56) Sieber, S.; Buzek, P.; Schleyer, P. v. R.; Koch, W.; Carneiro, J. W. d. M.; *J. Am. Chem. Soc.* **1993**, *115*, 259.

(57) Internet address: http://webbook.nist.gov.

(58) Berkowitz, J.; Ellison, G. B.; Gutman, D. *J. Phys. Chem.* **1994**, *98*, 2744.

(59) Cohen, N. *J. Phys. Chem.* **1992**, *96*, 9052.

(60) Szulejko, J. E.; McMahon, T. B. *J. Am. Chem. Soc.* **1993**, *115*, 7839.

(61) Seitz, C. F.; East, A. L. L. Unpublished work.

(62) Three examples would be refs 17 and 19 and the following: Collins, S. J.; O'Malley, P. J. *Chem. Phys. Lett.* **1994**, *228*, 246.